Biochemical Engineering Journal 203 (2024) 109211

Contents lists available at ScienceDirect

Biochemical Engineering Journal

journal homepage: www.elsevier.com/locate/bej

Regular article

Diluted methane mitigation by a co-culture of alkaliphilic methanotrophs and the microalgae *Scenedesmus obtusiusculus* towards carbon neutrality

Patricia Ruiz-Ruiz [a,b,d], Tania L. Gómez-Borraz [b,c,*], Alexis Saldivar [b], Sergio Hernández [b], Marcia Morales-Ibarría [b], Sergio Revah [b,**]

[a] Doctorado en Ciencias Naturales e Ingeniería, Universidad Autónoma Metropolitana-Cuajimalpa, Cd. de México, México
[b] Departamento de Procesos y Tecnología, Universidad Autónoma Metropolitana-Cuajimalpa, Av. Vasco de Quiroga 4871, colonia Santa Fe Cuajimalpa, C.P. 05300 Cd. de México, México
[c] School of Engineering, University of Glasgow, Glasgow, United Kingdom
[d] Center for Microbial Ecology and Technology (CMET), Faculty of Bioscience Engineering, Ghent University, Belgium

ARTICLE INFO

Keywords:
Microbial co-culture
Diluted methane
Carbon capture
Methanotrophic bacteria
Microalgae
Photonic pH control

ABSTRACT

A co-culture of an alkaliphilic methanotrophic consortium and the microalga *Scenedesmus obtusiusculus* was designed to consume CH_4 and CO_2 from diluted CH_4 streams under alkaline conditions to favor CO_2 retention. The highest CH_4 consumption rate in batch assays was 318 $mg_{CH4}\ g_{biomass}^{-1}\ d^{-1}$ with 8 % initial CH_4 and nitrate as the nitrogen source. Subsequently, the co-culture was evaluated in a photobioreactor with batch and fed-batch CH_4 feeds. Under continuous illumination, the CH_4 consumption rate reached 258 $mg_{CH4}\ g_{biomass}^{-1}\ d^{-1}$, but the pH increased to 9.8. After a photonic pH control implementation, the pH remained at 9.1 ± 0.05 with a consumption rate of 196 $mg_{CH4}\ g_{biomass}^{-1}\ d^{-1}$. The co-culture exhibited continuous activity, synchronized growth, and long-term stability, effectively removing both gases in a single reactor. Moreover, the co-culture's biomass showed an increase in reserve molecules, including carbohydrates and lipids, with protein as the primary product (40–52 % DCW), offering potential as a microbial protein source. The photonic pH control exhibited a rapid response, substituting the traditional acid/alkali addition method, which increases salinity, medium volume, and operational costs. The methanotroph-microalgae co-culture is a successful, robust, and stable alternative for diluted methane mitigation, resulting in nearly zero carbon emissions and valuable biomass production.

1. Introduction

The accumulation of greenhouse gases (GHGs) is a significant concern due to climate change. Methane (CH_4), with its high global warming potential (GWP_{100} = 28–34) and predominance in the atmosphere (global mean concentration of 1908 ppb in 2021) [1], is the second strongest contributor to GHG. It is generated by anaerobic processes, including solid waste and wastewater treatment, where the produced biogas is generally used for energy production as long as it meets certain conditions (above 20 % of CH_4 concentration and flux over 10 $m^3\ h^{-1}$ [2]). Unfortunately, these processes also generate a substantial amount of fugitive methane emissions, e.g. up to 40 % of produced CH_4 in an Upflow Anaerobic Sludge Blanket (UASB) can be dissolved in the effluent [3,4], as well as emissions from old landfills [5], known for its low CH_4 concentration and variable fluxes, that cannot be treated using conventional methods as flares, so alternative treatment approaches are required [6,7]. Additionally, carbon dioxide (CO_2) is also produced and released within these processes, increasing the net contribution of GHG to global warming.

Biological systems have demonstrated their viability in reducing CH_4 and CO_2 emissions under ambient conditions [8]. For CH_4, most reported methanotrophic bacteria metabolize it aerobically, yielding biomass, CO_2, and water. Under specific conditions (e.g. nitrogen or micronutrient limitation), they may produce a wide range of valuable products such as polyhydroxyalkanoates, methanobactin, exopolysaccharides, osmolytes, vitamins, etc. [9]. Photosynthetic prokaryotic and eukaryotic microorganisms (PM) may be used to further reduce GHG discharges by metabolizing the produced CO_2, generating biomass,

* Corresponding author at: Departamento de Procesos y Tecnología, Universidad Autónoma Metropolitana-Cuajimalpa, Av. Vasco de Quiroga 4871, colonia Santa Fe Cuajimalpa, C.P. 05300 Cd. de México, México.
** Corresponding author.
E-mail addresses: tania.gomezborraz@glasgow.ac.uk (T.L. Gómez-Borraz), srevah@cua.uam.mx (S. Revah).

https://doi.org/10.1016/j.bej.2023.109211
Received 24 October 2023; Received in revised form 19 December 2023; Accepted 27 December 2023
Available online 29 December 2023

and yielding O_2 as a byproduct. Photosynthetic microorganisms also have the potential to accumulate valuable products in their biomass, such as lipids and carbohydrates [10].

In nature, mixed microbial populations establish multiple positive, neutral, or adverse interactions, attaining dynamic equilibria. These systems offer some advantages over monocultures, such as an extended range of genes and metabolic capabilities, allowing the emergence of collective properties such as robustness and distribution of functions [11]. Under controlled conditions, methanotrophs and microalgae have been used in co-culture to improve nutrient recovery from wastewater and produce biomass [12], while other studies have explored utilizing CH_4/CO_2 mixtures, such as those in biogas, as the carbon source [13,14]. Consequently, the co-culture benefits from the synergy between the two components. The methanotrophic bacteria provide a source of CO_2 for the microalgae through methane oxidation, while the microalgae capture and utilize this CO_2, creating a cycle promoting both CO_2 retention and methane conversion. This is a sustainable alternative to remove both GHG and produce value-added compounds simultaneously.

Two processes need to be balanced to maximize the utilization of the carbon from CH_4 by the mixed methanotrophic-photoautotrophic systems. On the one hand, the growth of the methanotrophic bacteria, consuming CH_4 and O_2 and producing CO_2, and, on the other hand, the photosynthetic microbes requiring light to metabolize the inorganic carbon and replenish O_2. Initially, CH_4 requires high gas-liquid transfer rates to overcome its low solubility in aqueous media (dimensionless Henry's law constant is 30 at 25 °C) [15]. To foster the growth of the photosynthetic microorganism, the produced CO_2 can be retained in the liquid medium as carbonates under alkaline conditions [16]. Microalgae may use three different inorganic carbon assimilation pathways: (1) by direct CO_2 assimilation via the plasma membrane; (2) the use of bicarbonate by inducing the carbonic anhydrase enzyme, which converts HCO_3^- to CO_2; and (3) the direct bicarbonate transport via the plasma membrane [17]. Although not all PM can assimilate carbonates, there are reports of several *Scenedesmus* species able to grow with inorganic carbon sources such as $NaHCO_3$ and Na_2CO_3 [18]. Selecting alkaliphilic methanotrophic bacteria offers an interesting perspective as the growth conditions favor CO_2 retention and its subsequent uptake by the PM. Furthermore, it has been shown that alkaliphilic methanotrophs produce valuable compounds besides their biomass, such as ectoine and bioplastics [19].

Methanotrophs use different nitrogen (N) sources, including nitrate, urea, or ammonium salts, while only a few can fix N_2. The cellular mechanisms of sensitivity or resistance of strains to ammonium or nitrite are poorly characterized. Strain variability is substantial and probably influences the performance of the cultures [20]. Existing reviews describe the metabolism and assimilation paths of the primary nitrogen sources to sustain the growth of methanotrophic bacteria [21]. As with methanotrophic bacteria, microalgal growth also depends on nitrogen [22]. Consequently, selecting an appropriate nitrogen source is necessary to maintain an active syntrophy in the methanotrophic and photoautotrophic co-culture.

Previous studies indicated pH as one of the critical operating parameters due to its effect and dependence on the dissolution of gases and microbial metabolism [23,24]. The rate of CO_2 production by CH_4 catabolism directly affects the pH of the system as its dissolution causes acidification by forming carbonic acid, H_2CO_3. However, acidification can be reversed by the PM activity, which assimilates the produced carbonates, thereby increasing the pH. This enables a mechanism of pH control where light availability regulates the photosynthetic activity and the CO_2 balance in the system. The regulation of pH by controlling the illumination, photonic control, offers an alternative to maintain the activity of the mixed culture while avoiding changes in alkalinity and the increase in salinity, medium volume, and costs that occur when more traditional approaches to pH control involving alkali and acid addition are used.

Therefore, this study evaluated the capture of CH_4 from diluted methane in air, and the CO_2 produced thereof, with a co-culture of a bacterial alkaliphilic methanotrophic consortium and the microalga *Scenedesmus obtusiusculus*. Syntrophic growth was evaluated with two initial CH_4 concentrations and three N sources. Then, the co-culture performance was followed in a stirred tank photobioreactor in both batch and fed-batch CH_4 regimes, the latter in the long-term (>30 days) with a novel photonic pH control. The system was assessed by evaluating the gases and biomass kinetics, the relative methanotrophic-photoautotrophic activities, and the composition of the resulting biomass.

2. Materials and methods

2.1. Microorganisms and culture conditions

The alkaliphilic methanotrophic bacteria consortium (AMB) was enriched from soil samples of a former soda lake (Northern Latitude 19°30′52″ Western Longitude 98°59′24″, Texcoco Lake, near Mexico City). AMB was grown at 28 ± 1 °C in a 3-L glass-jacketed stirred tank reactor (Applikon Biotechnology, The Netherlands) with 1.5 L operation volume, fed with 5 % CH_4 in air (v v^{-1}) and mineral salts medium (MSM) containing (in g L^{-1}): $NaNO_3$, 2.0; $MgSO_4{\cdot}7H_2O$, 0.2; $FeSO_4{\cdot}7H_2O$, 0.001; Na_2HPO_4, 0.2; $NaH_2PO_4{\cdot}H_2O$, 0.09; KCl, 0.04; $CaCl_2{\cdot}2H_2O$, 0.015. The medium included the following trace elements (mg L^{-1}): $CuSO_4{\cdot}5\ H_2O$, 2.5; $ZnSO_4{\cdot}7H_2O$, 35; $NaMoO_4{\cdot}2\ H_2O$, 8.5; H_3BO_3, 5; $MnSO_4{\cdot}5H_2O$, 5; $CoCl_2$, 50. The pH was controlled between 9.0 and 9.5 with a 0.5 M NaOH solution. The main species in the AMB were reported by [24], including *Methylocystis* sp., *Methylomicrobium* sp., and *Methylophaga* sp. The unicellular microalga *Scenedesmus obtusiusculus* (PM), previously isolated from the wetlands of Cuatro Ciénegas and characterized by Refs. [23,25], was grown in a 5-L glass bubble column (0.1 m diameter and 0.64 m height) in a controlled temperature room (28 ± 2 °C) with 2.5 L operation volume in modified BG-11 medium containing (g L^{-1}): $NaNO_3$, 1.5; K_2HPO_4, 0.04; $MgSO_4{\cdot}7H_2O$, 0.075; magnesium disodium EDTA, 0.001; $CaCl_2{\cdot}2H_2O$, 0.036; citric acid, 0.006; ferric ammonium citrate, 0.006; Na_2CO_3, 0.02 and the following micronutrients (mg L^{-1}): H_3BO_3, 2.86; $MnCl_2{\cdot}4H_2O$, 1.81; $ZnSO_4{\cdot}7H_2O$, 0.222; $NaMoO_4{\cdot}2H_2O$, 0.39; $CuSO_4{\cdot}5H_2O$, 0.079; $Co(NO_3)_2{\cdot}6H_2O$, 0.494; pH 7.5. White LED lights were the illumination source with an average irradiance of 100 μmol m^{-2} s^{-1}. The incident irradiance on the glass bubble column surface was measured with a 2π quantum sensor (Extech, USA). Unless otherwise specified, the culture medium for the co-cultures in all experiments was prepared with a MSM:BG11 ratio of 3:1 (v v^{-1}) and with an inoculum of AMB:PM ratio of 3:1 (w w^{-1}) according to [24], which tested different proportions and concluded the 3:1 AMB:PM ratio presented the best performance in terms of CH_4 degradation rates.

2.2. Nitrogen sources and CH_4 concentration in microcosms assays

To evaluate the effect of the nitrogen sources and the CH_4 concentration on CH_4 consumption by the AMB-PM co-cultures, the assays were performed in 125 mL glass transparent serological bottles with butyl septa and aluminum crimp seals. The inoculation procedure was the same as reported previously [24] with 25 mL of liquid and 100 mL of headspace. Three different nitrogen sources were tested ($NaNO_3$, CO $(NH_2)_2$, and NH_4Cl) in MSM:BG11 (3:1 v v^{-1}) giving a concentration of 0.33 g_N L^{-1}. Two initial CH_4 concentrations, 4 % and 8 % (v v^{-1} in air), were set using a 20 mL syringe to inject a given volume of pure CH_4 (99 % v v^{-1}, Praxair, Mexico) into the headspace, just after removing the same volume of air to avoid overpressure in the glass bottles. Right after the injection, a sample from the headspace of all bottles was measured in a GC-TCD (Section 2.5). The initial pH was 9.15. Controls were done with the same nitrogen sources (0.33 g_N L^{-1}) using only AMB. Additional controls with only PM showed no methanotrophic activity. The bottles were placed horizontally in an orbital shaker at 400 rpm inside a

controlled temperature room (28 ± 2 °C). White LED lights provided an average irradiance of 115 μmol m^{-2} s^{-1}. CH_4 and CO_2 were monitored every hour by gas chromatography (GC-TCD), as described in Section 2.5. The kinetic assay duration was 24 h. pH and O_2 concentration were quantified at the end of the test. Due to the short duration and low initial CH_4 concentrations, biomass through DCW was not reported.

2.3. Stirred tank photobioreactor: batch experiments during continuous illumination or with photonic pH control

The co-culture was grown in a 3-L glass-jacketed stirred tank photobioreactor (STPR) (Applikon Biotechnology, The Netherlands) containing 1 L medium volume and equipped with a white LED strip light (Fig. S1), delivering an average internal irradiance of 110 μmol m^{-2} s^{-1} (measured inside the empty STPR). The initial AMB:PM biomass concentration was 1 ± 0.01 g L^{-1} (DCW), and NO_3 as the N source, which was selected from the microcosm experiments. The STPR operated in batch mode with an initial headspace CH_4 concentration of ~5 % (v v^{-1}); this concentration was selected for safety conditions considering the CH_4 Lower Explosive Limit (LEL). The pH and dissolved oxygen (DO) were measured with an electrochemical sensor (AppliSens, USA) and a polarographic DO sensor (AppliSens, USA), respectively. The data were acquired every second with a LabJack acquisition card. The temperature was controlled at 28 ± 1 °C using a PID controller with an electrical jacket installed around the LED strip, and agitation was set at 500 rpm. CH_4 and CO_2 concentrations in the headspace were measured every 10 min by GC-TCD as described in Section 2.5. For the photonic pH control test, the pH was maintained between 9.05 and 9.15 by automatic on-off switching of the LED illumination. The duration of both the continuous illumination test and the photonic pH control test was 8 h.

2.4. Stirred tank photobioreactor: fed-batch operation

The same STPR described above was used to assess the co-culture's long-term stability and robustness. The system was operated for 36 days with intermittent CH_4 feeding (fed-batch), giving CH_4 headspace concentrations ranging between 3–8 % (v v^{-1} in air) every 10 h. The AMB only control experiment was performed with 0.86 g L^{-1}. The co-culture inoculum contained an initial AMB:PM biomass concentration (DCW) of 0.61 ± 0.01 g L^{-1}. The reactor was operated at 28 ± 1 °C, 500 rpm, and initial pH of 9.5. The white LED illumination unit delivered an average internal irradiance of 150 μmol m^{-2} s^{-1}. The pH signal from the analog output of the sensor was connected to an Arduino nano® to regulate the microalgal activity through an on-off LED light control. Illumination switched off at pH 9.5 (avoiding thus an excessive increase in pH, [24]) and turned on again when the pH was below 9.4. Samples of the co-culture (50 mL) were drawn every three days, and the volume was replaced with the same amount of fresh MSM. Total biomass concentration was determined by DCW, and *Scenedesmus obtusiusculus* cell numbers were performed with a Neubauer-improved cell counting chamber. The macromolecular composition of the co-culture biomass (lipids, total carbohydrates, and proteins), total nitrogen, and soluble carbon were quantified by the methods described below. Concentrations of CH_4 and CO_2 were followed by GC-TCD to determine CH_4 consumption rates on specific days (1, 9 and 28).

2.5. Analytical procedures

CH_4 and CO_2 concentrations were measured in a thermal conductivity detector (TCD) gas chromatograph (6890 N Agilent) with a Porapak Q column. The injection volume was 500 μL with a gas-tight syringe, and helium was used as the carrier gas at 5 mL min^{-1}. The injector, detector, and oven temperatures were set at 110 °C, 200 °C and 50 °C, respectively. Final O_2 gas concentration on the microcosms assays was measured in a GC (GOW-MAC Series 550, USA) with TCD and a CTR1 column. The injection volume was 200 μL with a gas-tight syringe; He carrier gas flow rate was 100 mL min^{-1}, and the injector, detector, and oven temperatures were 50 °C, 115 °C and 50 °C, respectively. The pH was measured using an SG200C electrode (Sensorex, USA) at the end of microcosms assays (after 24 h).

Dry cell weight (DCW) was determined by vacuum filtering liquid samples of culture broth through a pre-weighted 0.2 μm pore size cellulose acetate membrane (Sartorius) followed by drying at 60 °C for 24 h. After this period, dry membranes were stored in a desiccation chamber and weighted at intervals of 1 h until constant weight.

The AMB and PM proportion in 10,000 recorded cells was obtained by size and complexity distribution through flow cytometry using a BD FACSCalibur (FACS, BD Bioscience, San José, CA). Sample preparation was the same as reported by [24]. Results were analyzed using FCS Express software version 7.06.0015 (DeNovo Software).

Protein and total carbohydrate analyses of the co-culture biomass were initiated by adding glass beads (0.5 g) to 1.0 mL co-culture samples and disrupting the cells with three 60-second cycles in a BeadBug® Microtube Homogenizer (Benchmark Scientific, USA). Protein content was determined with the modified Lowry method, and total carbohydrates with a modified phenol-sulfuric acid method [26]. Lipid content was quantified using the sulfo-phospho-vanillin method [27] from aliquots of 100–300 μL of the co-culture broth. The biochemical composition of biomass was expressed as DCW percentage.

Liquid samples of co-culture were filtered through a 0.2 μm pore size membrane prior to total carbon (TC) and inorganic carbon (IC) in a TOC-L CSH analyzer (Shimadzu, Japan) equipped with an infrared detection system (NDIR) through oxidative catalytic combustion method. Acidification was carried out using 0.1 M HCl, and the combustion temperature was 680 °C. Total organic carbon (TOC) was calculated as the difference between the measured TC and IC. Total nitrogen (TN) was determined in the same equipment coupled to a TNM-L chemiluminescence module for TN.

2.6. Calculations and statistics

Maximum specific CH_4 consumption rates (expressed as mg_{CH4} $g_{biomass}^{-1}$ d^{-1}) were calculated by adjusting the CH_4 consumption data, obtained by gas measurements during the kinetic assays, to the integrated Gompertz model and considering the DCW [28]. For gas calculations atmospheric pressure of Mexico City (0.75 atm) was considered. Theoretical CO_2 production was estimated using the molar CO_2 production yield obtained from the CO_2-produced/methane-consumed ratio in the microcosm assays using NO_3. Proton concentration during the batch stirred tank photobioreactor experiments was calculated from the measured pH values during the tests with the following formula: $[H^+] = 10^{-pH}$. Statistical analyses were done using SPSS 25.0 (IBM). Microcosms experiments were performed in duplicate, and results are presented as the average ± standard deviation. One-way ANOVA analysis was used to determine statistical differences in consumption rates with the different N sources and CH_4 concentrations; differences were considered statistically significant at $p \leq 0.05$.

3. Results and discussion

3.1. Effect of the N source and CH_4 concentration in microcosms assays

Table 1 shows the results of using three different nitrogen (N) sources and two initial CH_4 concentrations on the AMB controls and the AMB-PM co-cultures. Statistically significant differences were found in the CH_4 consumption rates between the three N sources tested and the initial headspace CH_4 concentrations used ($p \leq 0.05$). In the AMB controls, maximum specific CH_4 consumption rates with an initial 8 % CH_4 were around twice the value obtained with those having an initial 4 % CH_4 for each N source tested, as higher CH_4 gradients favor CH_4 solubilization, and therefore the uptake rates. Due to the respiratory activity, lower

Table 1
Results for AMB controls and the AMB-PM co-cultures for the microcosms assays with $NaNO_3$, $CO(NH_2)_2$ and NH_4Cl as N sources (initial N concentration 0.33 $g_N\ L^{-1}$).

Initial CH_4 (%)	Nitrogen source	Max. specific CH_4 consumption rate ($mg_{CH4}\ g^{-1}_{biomass}\ d^{-1}$)		Final pH*		Final O_2 (%)		Consumed CH_4 (%)	
		AMB	AMB-PM	AMB	AMB-PM	AMB	AMB-PM	AMB	AMB-PM
4	$NaNO_3$	301 ± 1.6	181 ± 3.7	7.2	11.0	14.4 ± 0.1	22.7 ± 3.1	89.9 ± 1.8	37.0 ± 5.1
8		606 ± 7.4	318 ± 9.8	7.0	11.0	3.2 ± 0.7	18.1 ± 1.9	97.6 ± 6.1	67.4 ± 6.8
4	$CO(NH_2)_2$	183 ± 0.8	60 ± 0.5	7.7	10.0	13.8 ± 0.3	23.8 ± 0.6	68.0 ± 2.0	11.6 ± 1.3
8		293 ± 1.2	72 ± 5.0	7.7	10.0	3.5 ± 0.1	22.3 ± 1.0	74.6 ± 2.1	10.4 ± 2.7
4	NH_4Cl	82 ± 0.9	39 ± 2.8	8.2	8.8	17.2 ± 1.0	19.8 ± 1.1	5.6 ± 0.6	6.4 ± 1.7
8		174 ± 2.0	40 ± 10.7	7.4	8.8	7.3 ± 0.9	19.0 ± 0.7	49.0 ± 0.7	4.3 ± 0.4

* Note: The standard deviation for the pH in all cases ranged between ± 0.3 % of error. The final biomass is not reported as non-significant differences were found with the initial values due to short experiment duration (24 h).

final O_2 concentrations were found with increased CH_4 uptake. The highest CH_4 consumption rate was 606 $mg_{CH4}\ g^{-1}_{biomass}\ d^{-1}$ with 8 % CH_4 and NO_3^- as the N source. Similar CO_2 molar yields (average 0.79 ± 0.04 $mol_{CO2}\ mol^{-1}_{CH4}$) were obtained with NO_3^- for both 4 % and 8 % initial CH_4, as shown in Table 1. In contrast to NO_3^-, urea and NH_4^+ had lower CH_4 consumption rates, which is consistent with soil experiments [29,30]. Although NH_4^+ can be more easily assimilated than NO_3^- by its incorporation into the amino acids, it can also have an inhibitory effect on some methanotrophs [31] because the methane monooxygenases, MMO, have relatively low substrate specificity and can oxidize NH_4^+ to the toxic intermediate hydroxylamine [20]. Experiments on axenic strains [32,33] as well as in soil microcosms [30,34] have shown that NH_4^+ concentrations as low as 5 mM and 17 mM are enough to inhibit CH_4 uptake rate which may explain the decrease in methanotrophic activity. Moreover, as ammonia has a pKa of 9.2, free ammonia, which is known to have inhibitory effects [35], could represent about 50 % of the total nitrogen concentration in the experiments. Lower CH_4 removal rates, (around 50–60 %) with urea by the AMB consortium could be explained by the activity of the urease enzyme that enables the conversion of urea into NH_4^+ with the inhibitory effect described above, [29]. Besides the NH_4^+ inhibition, it has the drawback that it may be stripped as NH_3 in alkaline conditions and open systems. Moreover, due to the short-term duration of the experiments (24 h) the biomass production between the three N sources was not significant. Theoretical calculations considering the initial and final carbon from CH_4 and CO_2 in both gas and liquid phases, estimated that up to 20 % of the consumed carbon was incorporated into biomass after 24 h in the AMB-PM co-culture with nitrate and 8 % of initial CH_4.

The pH decreased in the AMB controls, due to the produced CO_2, to levels where the methanotrophic activity was reduced and eventually inhibited. The alkaliphilic consortium, adapted to a pH between 9.0 and 9.5, was inhibited as pH approached 7. The lowest values registered for pH were close to 7.0 with NO_3^-. The pH may also change due to variations in the ionic balance in the medium induced by microbial growth. It is well known that NO_3^- uptake favors the increase in pH by sequestering H^+, and, in contrast, NH_4^+ consumption tends to release H^+ and hence to acidify the medium. Despite these observations, the higher pH reduction in the AMB controls against the AMB-PM co-culture (as shown in Table 1) suggests that CO_2 accumulation (2.52 % and 6.63 % produced CO_2 for 4 % and 8 % CH_4 concentration, respectively) was the main pH driver.

Table 1 also shows that the concurrent activity of AMB and PM populations led to an initial 40–50 % reduction in methanotrophic activity. The reduced activity was consistent with the previous report by [24]. [36] also found this trend in the first 24 h of experiments combining methanotrophs and microalgae in diluted digestate using biogas (without air/oxygen addition), although an increase in both CH_4 assimilation and CO_2 fixation was observed after 48 h. Similarly, other studies utilizing biogas have found a mutualistic relation between methanotrophic bacteria and photosynthetic microorganisms in the long term [37]. The reduced methanotrophic activity, which deserves further study, could be associated with organic molecules in the culture medium excreted by *S. obtusiusculus* (PM), such as extracellular polymeric substances or photosynthates [38], influencing the CH_4 metabolism or its transfer. It is well known that various molecules may inhibit methanotrophic bacteria [39,40]. In this sense, the continuous enrichment of the AMB under the selected co-culture conditions may allow for overcoming this limitation, as reported previously [24].

As in the AMB controls, NO_3^- sustained the highest CH_4 consumption rate in the co-cultures (318 $mg_{CH4}\ g^{-1}_{biomass}\ d^{-1}$ with 8 % CH_4) compared to the other N source treatments. As well as with the methanotrophs, previous studies have also found that the N source can affect the microalgal growth of axenic cultures, although results are strain dependent [22]. Slower rates with extreme final pH explain the reduction in the global CH_4 consumption. NO_3^- favored the activity in co-cultures and presented the highest CH_4 consumption rate, raising the final pH to around 11, which may be close to the upper limit for the bacteria. Globally, *S. obtusiusculus* (PM) increased the pH due to the CO_2 uptake and produced O_2 in the process (19- 24 % of gaseous O_2). The higher pH may also reflect the increased H^+ uptake by *S. obtusiusculus* (PM). As in the controls, nitrogen in the medium, as ammonium salt, had a deleterious effect which may have been further aggravated as the higher pH in the co-cultures favored a higher ammonia concentration (pKa = 9.2), which is itself inhibitory as described previously. [41] observed a 30 % reduction in the final cell mass for *Scenedesmus* cells for concentrations ranging between 200 and 500 ppm NH_4^+, and a drastic decrease (>60 %) when it was above 800 ppm NH_4^+. While *Dunaliella* showed a similar trend, other species, such as *Chlorella,* showed that, even if they were not inhibited by NH_4^+, had growth rates up to 1.75 times higher when using NO_3^- instead [42]. Interestingly, the results with urea show a higher final O_2 concentration, which can be associated with increased CO_2 availability due to its content in the urea molecule. The headspace CO_2 was only detected with NH_4^+ (results not shown), facilitated by the equilibrium displacement due to the lower pH. In the other co-culture assays, the CO_2 produced was assimilated or remained as carbonates in the alkaline medium (pH > 8.8), available to be further biodegraded by the PM.

The experiments confirmed that NO_3^- was the most effective N source promoting the syntrophy of the co-culture under the alkaline conditions used in this study. They also prove that pH control is necessary to balance the methanotrophic and photoautotrophic activities; this will be attained using light to control the photosynthetic activity and hence, the CO_2 and carbonates uptake.

3.2. Stirred tank photobioreactor experiments

3.2.1. Batch without pH control (continuous illumination)

The co-culture in the stirred tank photobioreactor allowed homogeneous suspended growth without granulation, in contrast to other reports [37] where macroscopic granules are formed due to the filamentous nature of the photoautotrophic organism used. The CH_4 and CO_2 content in the reactor headspace are shown in Fig. 1a; the figure also indicates the estimated CO_2 calculated from the CH_4 oxidation yield (0.79 $mol_{CO2}\ mol^{-1}_{CH4}$) of the microcosm assays (AMB and NO_3^-). It was

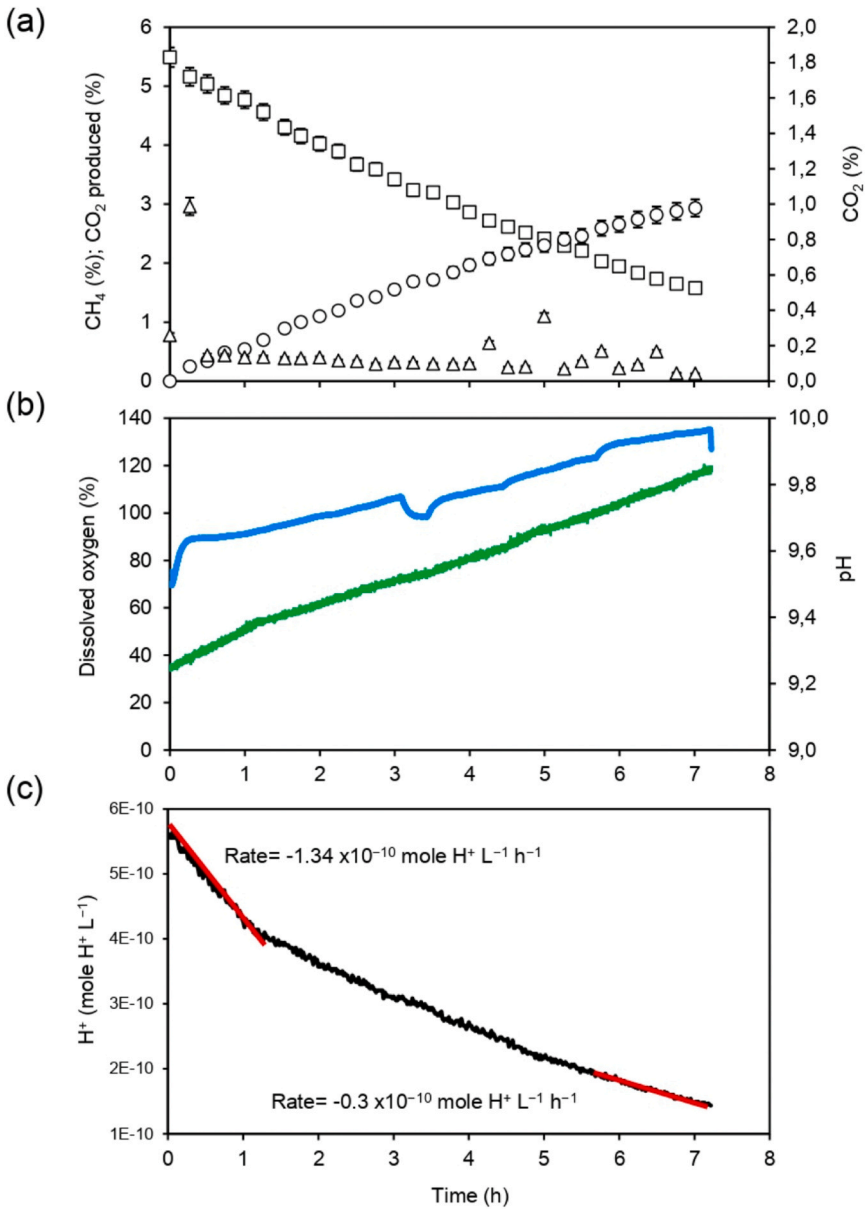

Fig. 1. Data of the STPR with the AMB-PM co-culture during the batch continuous illumination experiment. (a) CH_4 (square) and CO_2 (triangle) concentration in the headspace and estimated CO_2 (circle) production; (b) pH (green line) and dissolved oxygen evolution (blue line). (c) Proton evolution in the STPR.

observed that, while the average headspace CO_2 was 0.13 ± 0.07 %, it had a decreasing tendency (to <0.1 %), even though CO_2 was continually produced (estimated production rate, 482 mg_{CO2} $g_{biomass}^{-1}$ d^{-1}), reflecting the consumption by *S. obtusiusculus* (PM), and the equilibrium displacement to carbonates due to the increased pH. The maximum specific CH_4 consumption rate, obtained at around 3 h, was 258 mg_{CH4} $g_{biomass}^{-1}$ d^{-1}, which was 1.4-fold higher than the AMB-PM in microcosms at similar conditions (4 % CH_4, 181 ± 3.7 mg_{CH4} $g_{biomass}^{-1}$ d^{-1}).

Fig. 1b shows that pH increased from 9.2 to 9.85 in approximately 7 h, following the same trend as the microcosm experiments, thus confirming the need to control pH within the optimal range of 9.0–9.5. The DO decline at the end of the experiment occurred once the light had been turned off. [23] reported the optimum photosynthetic activity for *Scenedesmus obtusiusculus* (PM) at around pH 8 and a 65 % reduction at pH 9. From the microcosm experiments depicted in Table 1, a rise in pH above 10 may be expected in long-term cultivations without pH control, which will be unfavorable for both the CH_4 and CO_2 uptake. Although the pH shows a steady increase, alkalinization is better represented by the proton concentration (H^+), calculated from the pH data, and presented in Fig. 1c. The proton production rates, calculated from the slope, show that proton uptake slows as time evolves, from -1.34×10^{-10} mole H^+ L^{-1} h^{-1} to -0.3×10^{-10} mole H^+ L^{-1} h^{-1}. The decrease could be associated with the medium alkalinization and the reduction of the CH_4 concentration.

DO in the system increased from 60 % to 140 %, or around 8.4 mgO_2 L^{-1} at the atmospheric pressure of Mexico City, due to the microalgal activity, favoring CH_4 oxidation by methanotrophic bacteria. Nevertheless, high DO levels could inhibit microalgae activity and must be monitored and controlled [23,25,43], especially in batch or semi-batch assays. For *S. obtusiusculus* (PM), only DO above 20 mgO_2 L^{-1} has an inhibitory effect on the photosynthetic activity [23].

The relative methanotrophic-photoautotrophic activities were estimated by the O_2 produced and the CO_2 consumed. Table 2 shows the molar equilibrium based on the gas mass balances in the liquid and gas phases and the microbial growth rate. The methanotrophic activity was determined considering the AMB consortium yields obtained from the microcosm assays (0.79 mol_{CO2} mol_{CH4}^{-1} and 1.84 mol_{O2} mol_{CH4}^{-1}) and the CH_4 and CO_2 measurements in the gas phase. Photoautotrophy

Table 2
Individual consumption/production (estimated) and overall (AMB-PM) CO_2 and O_2 balances in the STPR for the batch continuous illumination experiment.

	Total mmol	
	CO_2 balance	O_2 balance
AMB	+ 94	-219
PM	-101	+ 272
AMB-PM	-7	+ 53

*Negative values represent consumption; positive values mean production/accumulation.

estimation included the CO_2 in the gas phase, the carbonate equilibrium with the pH, and the DO. Results demonstrated that PM seemed to predominate in the global AMB-PM activity. One of the main reasons is the different bioavailability of the gaseous components in the aqueous medium. While low CH_4 solubility limits methanotrophic activity, the alkaline pH favors CO_2 retention and, consequently, PM metabolism. The CO_2 balance resulted negative in the co-culture, as carbon uptake from PM included not only the CO_2 produced by CH_4 oxidation but also the initial inorganic carbon content.

The evolution of the population in the STPR was observed by flow cytometry. As mentioned previously, a 3:1 AMB-PM ratio was inoculated in the experiments at the STPR. Fig. 2 shows that the AMB:PM proportion remained practically constant in the initial and final samples. This suggests this ratio was adequate, as the microcosms assays indicated, and was appropriate when the system was scaled-up. It is also important to mention that the relative abundance of AMB does not reflect the actual mass proportion as the mass of individual AMB cells (average size of 0.5–4.0 × 0.5–2.0 μm) [21] is much lower than that of *S. obtusiusculus* (PM) (4.8 μm width × 13.2 μm length) [25].

3.2.2. Batch with photonic pH control

The pH control based on intermittent illumination to regulate the CO_2 content was studied in the same photobioreactor. The rapid response reflects previous results by [44], who reported the dynamics of photobioreactors to irradiation changes. The headspace CH_4 concentration decreased to 1.75 % v v^{-1} (Fig. 3a) with a constant consumption rate around 196 $mg_{CH4}\ g_{biomass}^{-1}\ d^{-1}$ and was not affected by the exposure to light-dark phases as AMB activity was not light dependent. Previous reports indicate that light exposure does not affect CH_4 uptake rates in methanotrophic bacteria [45]. Moreover, [46] recently measured the relative abundance and RNA transcripts related to aerobic methanotrophic activity and confirmed that light does not significantly affect aerobic methanotrophic bacteria in coastal sediments.

The gaseous CO_2 remained at 0.22 ± 0.04 % and showed slight variations during the illumination cycles. With light, the CO_2 removal by PM was faster than the CO_2 produced by the AMB, indicating a lower CO_2 gaseous content. The opposite occurs in the dark phase, where the CO_2 increases almost at the same initial level of the experiment. The pH control shown in Fig. 3b favored minor variations in the headspace and, consequently, in the liquid medium. The average headspace value (0.22 ± 0.04 % CO_2) was higher than in the uncontrolled assay (0.13 ± 0.07 % CO_2), probably due to the lower pH in this experiment.

The effect of the illumination cycles on pH and DO (Fig. 3) shows that at the beginning of the operation, when CH_4 was more concentrated, the initial DO was at 80 % saturation, reaching 95 % by the action of *S. obtusiusculus* (PM). On/ off switching of the lights elicited a fast response (~5 s). As the AMB consortium removed the CH_4, the DO concentration during the light periods reached levels that exceeded the 100 % saturation value of the medium after the second hour of operation. The lowest levels recorded during the dark periods were maintained at approximately 40 %. This shows that there was no oxygen deficiency in the system due to the presence of PM culture, which removes most of the CO_2 produced, allowing the sequestration of both gases within a single system. Table 3 summarizes the specific and global oxygen-consuming trend by the methanotrophic consortium, considering the 3:1 biomass ratio (only 75 % of the total biomass is methanotrophic bacteria). The mean value for the duration of each dark period was 0.35 h, while the global oxygen uptake (consumption) rate was 822 ± 110 $gO_{2consumed}\ m^{-3}\ d^{-1}$ or 0.88 $gO_{2consumed}\ g_{biomass}^{-1}\ d^{-1}$.

With respect to the pH evolution, shorter periods were found for the acidification step (i.e., dark phase with only CO_2 production). The proton concentration (H^+) was calculated from the pH data and represented in Fig. 3c. From these values, the proton production rates were calculated (Table 4) for each period yielding average rates of − 3.07 ± 0.85 × 10^{-10} and + 5.28 ± 0.54 × 10^{-10} mole $H^+\ L^{-1}\ h^{-1}$ for the illuminated and dark phases, respectively. The value for the first period with light was consistent with the result obtained in the experiment with continuous illumination (rate = 1.34 ×10^{-10} mole $H^+\ L^{-1}\ h^{-1}$). These values show that, during the illuminated phase, algal activity overcomes that of bacteria until the following dark phase. The AMB-PM populations could theoretically show balanced growth and thus maintain a stable pH. However, in practice, the relative volumetric rates diverge due to differences in growth rates, cell numbers, susceptibility to organic molecules, shading effects, etc. Although the CO_2/carbonates equilibrium mainly determined the pH, other factors have an influence, such as

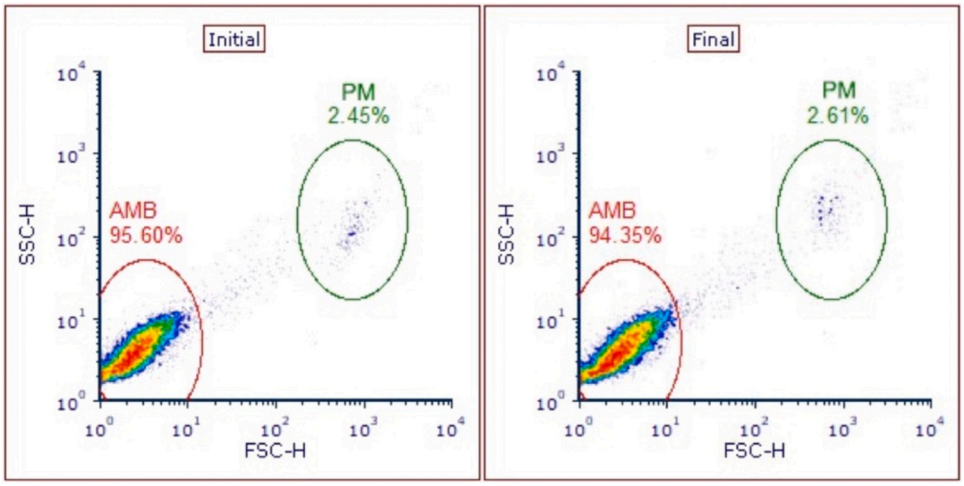

Fig. 2. Enumeration of each cell type from 10,000 recorded cells via size and complexity of the initial and final AMB-PM biomass inside the STPR during the batch continuous illumination experiment; side scatter (SSC) is plotted against forward scatter (FSC). The percentage of alkaliphilic methanotrophic bacteria (AMB) and microalga *Scenedesmus obtusiusculus* (PM) are shown.

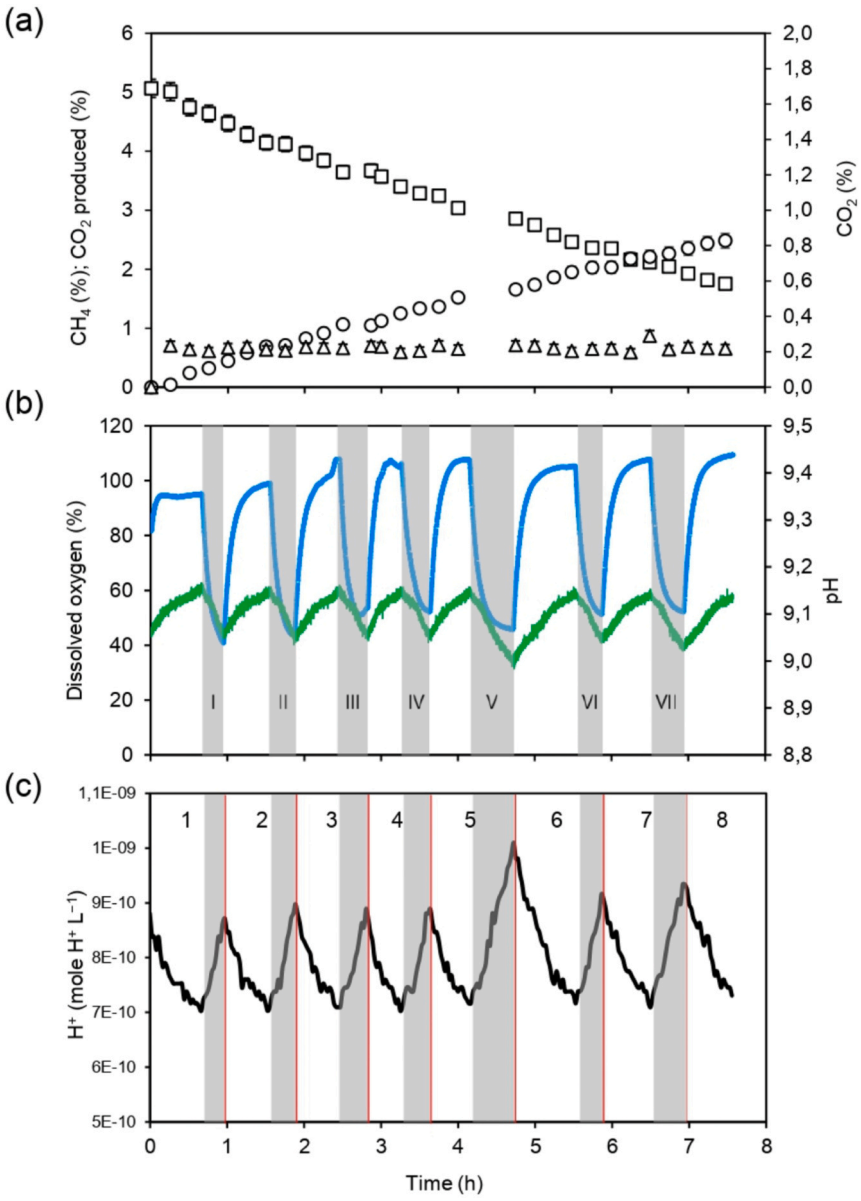

Fig. 3. Data of the STPR with the AMB-PM co-culture under the batch photonic pH control experiment. (a) CH_4 (square) and CO_2 (triangle) concentration in the headspace and estimated CO_2 (circle) production; (b) pH (green line) and dissolved oxygen evolution (blue line). Dark phases are indicated as I-VII. (c) Proton evolution in the STPR and complete light/dark periods are indicated as 1–8.

Table 3
Dissolved oxygen variations and rates in the STPR during the batch photonic pH control experiment.

Period	Duration (h)	DO min (%)	DO max (%)	$gO_{2consumed}\ g_{biomass}^{-1}\ d^{-1}$	$gO_{2consumed}\ m^{-3}\ d^{-1}$
I	0.29	40.64	95.37	0.78	730.00
II	0.32	43.80	99.44	0.77	712.54
III	0.37	50.55	108.20	1.06	986.84
IV	0.36	51.77	107.65	0.77	713.52
V	0.57	45.57	107.89	1.00	932.62
VI	0.34	51.10	105.58	0.87	812.72
VII	0.44	52.07	107.89	0.93	866.23

Table 4
Proton production rate for the batch photonic pH control experiment. Rates are expressed as mole H^+ $x10^{-10}$ L^{-1} h^{-1}.

Period →	1	2	3	4	5	6	7	8
Light	-2.02	-2.69	-3.25	-3.72	-3.16	-3.47	-2.99	-3.27
Dark	5.64	5.58	4.67	4.90	5.25	5.75	5.19	

nitrate uptake or the production of other molecules, such as organic acids [38].

Similar to the previous flow cytometry assay, Fig. S2 shows that the 3:1 AMB-PM ratio allowed balanced growth between both microbial groups and maintained stability in the system as the activity (CH_4 consumption; and CO_2 and O_2 production and consumption) was not affected inside the STPR.

The photonic pH control method was easily implemented, showed a fast response, and eliminates the problems associated with the traditional technique of acid/alkali additions, which includes the costs and storing of the chemicals, the increased salinity, the dilution effect, and complications that may arise from poor mixing, such as hotspots.

3.2.3. *Fed-batch operation*

Co-culture biomass production and nitrogen evolution, in Fig. 4 and

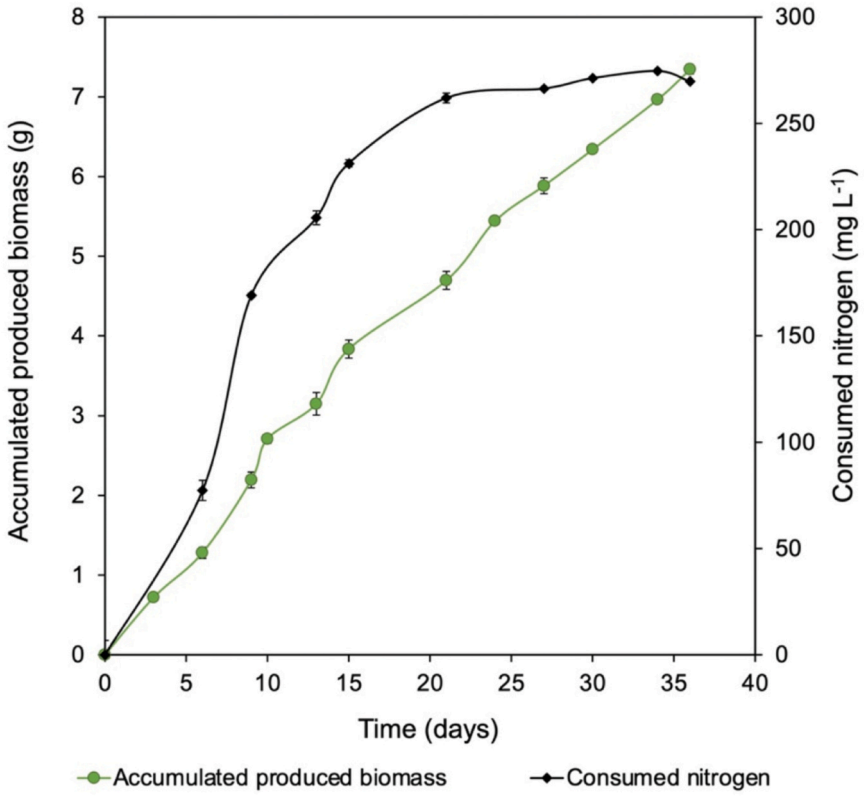

Fig. 4. Accumulated produced biomass considering biomass withdrawals (green line) and consumed nitrogen (black line) during fed-batch (long-term) co-culture operation.

S3, show constant biomass accumulation, attaining a final concentration of 3.68 ± 0.05 g L^{-1} on day 36. The cell count of *S. obtusiusculus,* in Fig. S4, shows constant growth until day 21, which coincides with the beginning of N limitation in the culture medium which restricts cell duplication but favors the accumulation of reserve materials. Also, microalgal numbers in Fig. S4 follow a similar trend a the DCW in Fig. S3 suggesting that the AMB:PM proportion did not significantly changed. The total accumulated produced biomass was 7.34 g considering the biomass removed in the periodic medium replenishments. AMB-PM maximum biomass concentration was lower than the 4.16 g L^{-1} obtained by the single cultivation of *Scenedesmus obtusiusculus* in indoor-controlled conditions, N-replete medium, and no CO_2 or light limitations [23], but higher than other methanotrophic-microalgae suspended co-cultures in bottles (3 g L^{-1}, [36]; 1.48 g L^{-1}, [12]; 0.8 g L^{-1}, [13]). However, in some of these studies, biogas was used as the carbon source, and oxygen availability depended solely on the activity of the photosynthetic microorganism. Additionally, wastewater was used besides the mineral medium. In this situation, the effluent may lack essential nutrients or contain molecules that may inhibit the growth of both microalgae and methanotrophs. In our study, supplementing fresh medium after sampling provided the required nutrients for sustained growth.

In the initial days, under nitrogen-replete conditions, the biomass yield per gram of N consumed was 16.26 $g_{biomass}$ $g^{-1}_{Nconsumed}$, or an expected 6.2 % nitrogen content in the biomass, which was obtained from the calculated slope depicted in Fig. S5. The limiting N concentration was 27.7 mg L^{-1} when the system reached 2.66 $g_{biomass}$ L^{-1} on day 21. After this period, nitrogen availability was determined from the added fresh medium (14.4 mg_N L^{-1}). These nitrogen-depleted conditions favored the accumulation of reserve molecules, which will be discussed later.

The CH_4 consumption and CO_2 production of AMB alone (Fig. 5a), and AMB-PM (Fig. 5b, c, and d), were used to calculate CH_4 consumption rates at specific days of operation. The CH_4 consumption rate of the AMB culture alone was 262 mg_{CH4} $g^{-1}_{biomass}$ d^{-1}. Similarly, the AMB-PM consumption rate on day 1 was 251 mg_{CH4} $g^{-1}_{biomass}$ d^{-1}, practically the same as the AMB-PM experiments operated on batch mode with continuous illumination (258 mg_{CH4} $g^{-1}_{biomass}$ d^{-1}) and higher than rates with photonic pH control (196 mg_{CH4} $g^{-1}_{biomass}$ d^{-1}). AMB-PM specific CH_4 consumption rates were 86 and 37 mg_{CH4} $g^{-1}_{biomass}$ d^{-1} on days 9 and 28, respectively. Although these rates were lower compared to the rates at the beginning of the co-culture, headspace measurements before each CH_4 cycle-feeding showed that the co-culture depleted all the CH_4 fed to the system in less than 10 h, as no CH_4 or CO_2 were detected in the headspace. Volumetric CH_4 consumption rates, Fig. 5, show that the highest co-culture rate was on the ninth day (212 mg_{CH4} L^{-1} d^{-1}), comparable to AMB, with an average consumption rate of 162 $mgCH_4$ L^{-1} d^{-1} for the entire experiment. The rates attained by the co-culture in the STPR were higher (except for day 28) than those in microcosms with 4 % of CH_4 and $NaNO_3$ as N source (136 mg_{CH4} L^{-1} d^{-1}), demonstrating the benefit of using stirred tank photobioreactors to improve mass gas transfer, especially of the sparingly soluble CH_4. In this case, the stirring rate was set at 500 rpm. The rates are also higher than those with photogranules in reactors constructed to remove dissolved CH_4 from anaerobic effluents as reported by Ref. [37], of 26.3 ± 2.6 mg_{CH4} L^{-1} d^{-1}, probably due to the increased mass transfer favored by higher agitation and unicellular (vs granular) cell development.

Fig. S6 shows the pH recorded during the operation. The co-culture was exposed to different CH_4-feeding concentrations to test its stability. When the CH_4 concentration was below 5.5 %, the pH remained between 9.1 and 9.5 (Fig. S6), and CO_2 was negligible in the gas phase (Fig. 5b), implying that it was consumed/retained in the culture medium. However, when a higher CH_4 concentration was fed to the system (~8 %), it resulted in more CO_2 production via methanotrophs, causing medium acidification and, therefore, a decrease in pH, which dropped to 7.8 and remained between 7.8–8.5. During this period, and confirmed

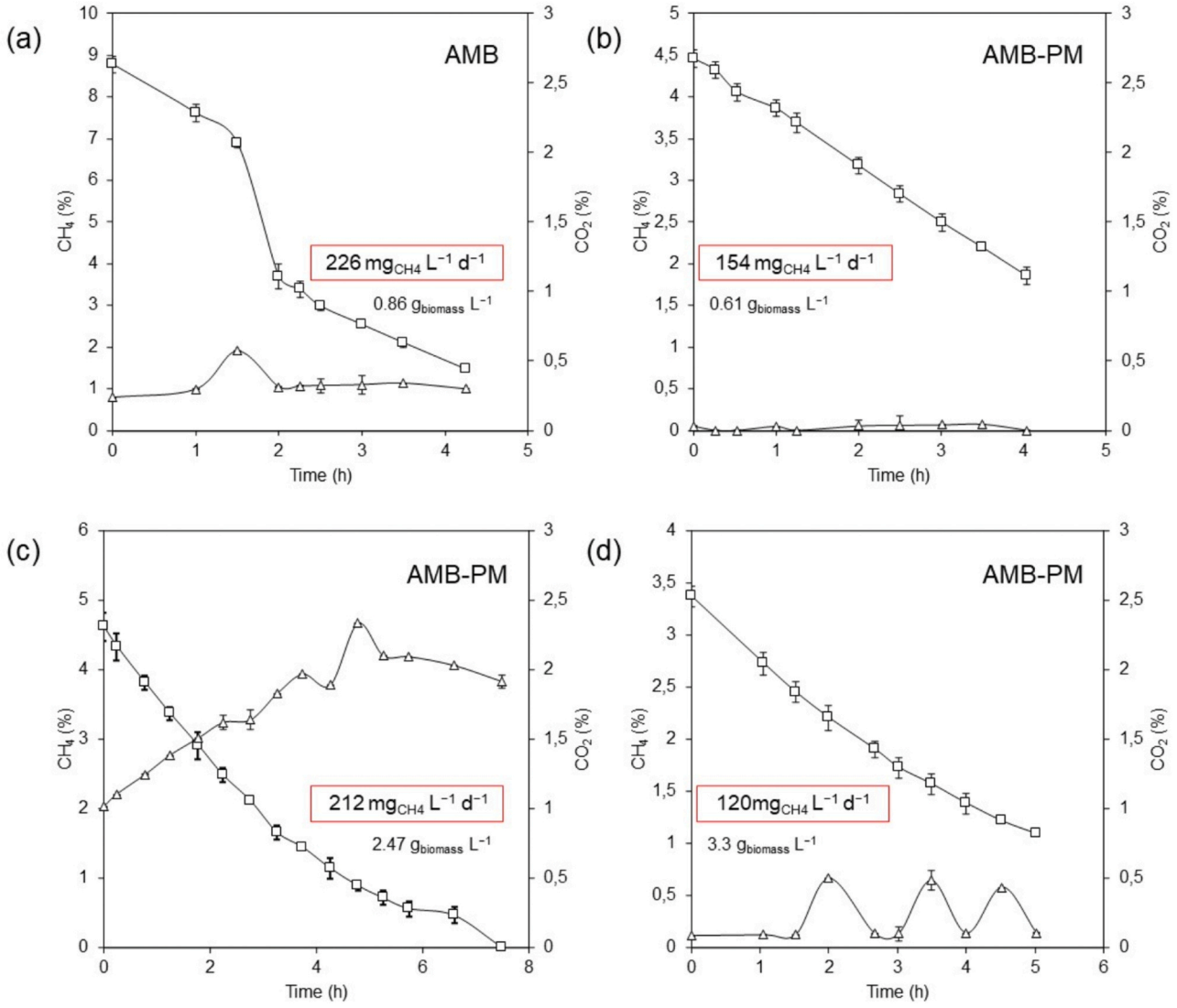

Fig. 5. Gas phase composition on different operation days during fed-batch (long-term) co-culture operation. CH_4 (square) and CO_2 (triangle) concentration in the headspace. (a) AMB consortium alone; (b) Co-culture on day 1; (c) Co-culture on day 9; (d) Co-culture on day 28. CH_4 volumetric consumption rates and biomass concentrations are indicated.

by kinetic data on day 9, CO_2 was detected in the gas phase, increasing to reach a maximum of 2.3 % (Fig. 5c). Then, it started to decrease, which can be explained by the CO_2/carbonates equilibrium. From day 14, the CH_4 feed concentration was reduced to 3–5 %, and with this, the system retrieved its stability, maintaining the pH between 9.4 and 9.5 through the light on/off control. Finally, from day 27, CH_4 feed concentration was increased to 7–8 %, showing a slight drop in pH, but this time it remained around 9. Despite pH changes driven by the CH_4 concentration fed, the system did not lose the ability to oxidize CH_4. In this study, feeding concentrations of 3–5 % of CH_4 allowed higher stability with the photonic pH control. For safety reasons, a full-scale system must preferably be operated below the LEL to avoid explosion risks.

Soluble carbon measurements (TC, IC, and TOC, see Fig. S7) at selected days showed that TC initially increased up to a value around 400 mg L^{-1} after day 9, of which more than 75 % corresponds to IC, and the rest is TOC. As no organic matter was added to the medium, this was exclusively released by the AMB or *S. obtusiusculus* (PM). Some studies confirmed that methanotrophs may excrete a significant amount of organic matter (i.e., acetate, formate, citrate, and succinate) during formaldehyde assimilation [47]. [13] reported the release of dissolved organic carbon by *Methylocystis bryophila,* which was further consumed in co-culture by *Scenedesmus obliquus*. These authors found that genes related to organic metabolism were upregulated, establishing that acetate released by *M. bryophila* may be the primary carbon source for the mixotrophic growth of *S. obliquus*. Other studies have also reported the growth of *Scenedesmus* with acetate as the main carbon source [10,48] and other microalgae genera such as *Desmodesmus* or *Chlorella* [49]. Results in the present study show a significant amount of inorganic carbon retained in the medium (maximum of 358 mg L^{-1}) and organic carbon in a smaller proportion (95 mg L^{-1} on average). The fact that the soluble carbon remains relatively constant, despite the biomass increase, suggests that equilibrium was established between produced and consumed organic molecules by the highly diverse heterotrophic bacteria present in the AMB consortium [24] such as *Alishewanella* sp., *Halomonas* sp., *Dokdonella* sp. and bacteria of the phylum Gemmatimonadetes, among others, with the autotrophic and mixotrophic growth of the photosynthetic microorganism.

The composition of the co-culture biomass was determined to identify possible applications of the produced biomass. As seen in Fig. 6, early growth in the rich initial medium favors a higher protein content that is reduced as the medium becomes limited (i.e. nitrogen limited) once it is added intermittently. Limited nutrient availability promoted

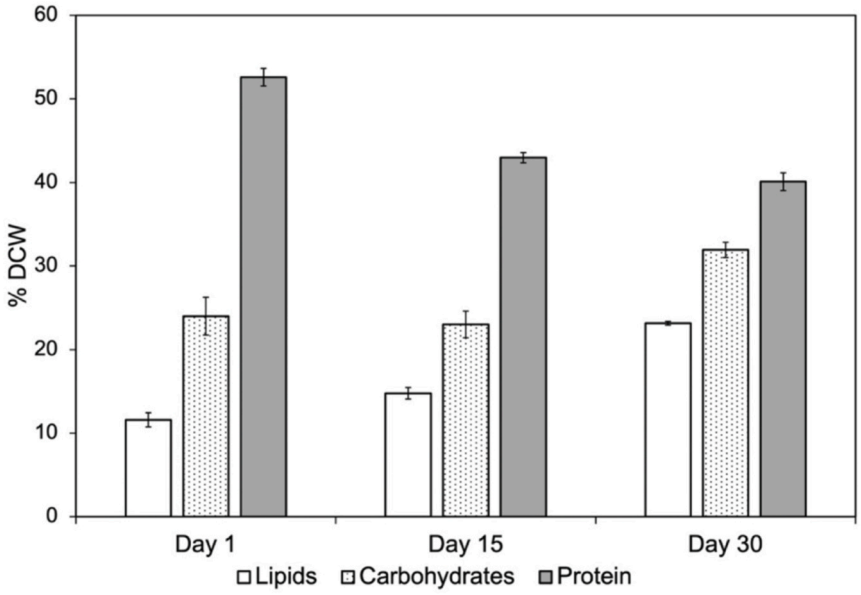

Fig. 6. Co-culture macromolecular composition during fed-batch (long-term) operation. Ultimately, it was demonstrated that the AMB-PM co-culture using photonic control could thrive and reach a stable long-term operation to produce valuable-high products, such as biomass directly, or induce nutrient limitation for other molecules accumulation (lipids, PHB).

the accumulation of reserve molecules such as carbohydrates and lipids, attaining 31.9 % DCW and 23.2 % DCW, respectively, on day 30. Although PHB was not measured in this study, it is also important to consider it as another possible reserve material since it is well-known to be one of the major reserve compounds produced by methanotrophic bacteria. On the other hand, *Scenedesmus obtusiusculus* has been previously reported for lipid production under nitrogen limitation, reaching values ranging from 45–55 % DCW [25]. However, the lipid content of the co-culture in this study was much lower, suggesting that co-culture biomass may not be suitable for biofuel production. Instead, various reports [12,36] indicate that the co-culture biomass of methanotrophs and microalgae could be a promising source for microbial protein for animal feed, as is the case for the 40–52 % DCW of protein obtained in this study. Nutritional studies focusing on the digestibility and amino acid profile of the co-culture biomass must be carried out prior to using the biomass for this purpose.

4. Conclusions

The study showed that efficient consumption of CH_4 and CO_2 from diluted methane, with constant biomass production, can be maintained for long periods by a co-culture of a bacterial alkaliphilic methanotrophic consortium and the microalga *Scenedesmus obtusiusculus*. Nitrate favored the syntrophy of the co-culture, allowing for the highest CH_4 uptake rates. Photonic pH control proved to be an advantageous method to maintain the continuous activity of the mixed culture, with no significant changes in the relation of the AMB or PM populations (cell counting by flow cytometry) during the STPR experiments.

Fed-batch operation allowed the depletion of the added CH_4 and maximized biomass production. The long-term operation showed that the soluble inorganic and organic carbon concentration in the medium attained an equilibrium between production and autotrophic and heterotrophic consumption. The proximate composition of the co-culture showed the accumulation of reserve materials, such as carbohydrates and lipids, as the nitrogen source availability was reduced.

The co-culture of methanotrophs and photoautotrophs provides an alternative method contributing to both diluted methane mitigation and carbon dioxide sequestration, simultaneously addressing two critical environmental concerns, with nearly zero carbon emissions leading towards a carbon neutrality process. Further process improvement may include adding specific on-line sensors (carbonates, nitrates), automating CH_4 addition, advanced regulation of the light intensity to maximize both the methanotrophic and photoautotrophic activities, controlling the biomass composition through regulated medium addition, and on-line measurement of the bacterial and microalgal biomass ratio. An additional challenge is to integrate sunlight periods into the process to improve its economy.

CRediT authorship contribution statement

Tania L. Gómez-Borraz: Conceptualization, Formal analysis, Investigation, Methodology, Writing – original draft, Writing – review & editing. **Alexis Saldivar:** Investigation, Methodology, Software. **Patricia Ruiz-Ruiz:** Conceptualization, Formal analysis, Investigation, Methodology, Writing – original draft, Writing – review & editing. **Marcia Morales-Ibarría:** Funding acquisition, Project administration, Resources, Supervision. **Sergio Revah:** Conceptualization, Funding acquisition, Project administration, Resources, Supervision, Writing – review & editing. **Sergio Hernández:** Methodology, Resources.

Declaration of Competing Interest

The authors declare that they have no known competing financial interests or personal relationships that could have appeared to influence the work reported in this paper.

Data availability

Data will be made available on request.

Acknowledgements

This study was funded by the CONAHCyT project PDCPN 2015-241. Ruiz-Ruiz also thanks CONAHCyT for the scholarship for her doctoral studies (CVU 661471).

Appendix A. Supporting information

Supplementary data associated with this article can be found in the online version at doi:10.1016/j.bej.2023.109211.

References

[1] R.B. Skeie, Ø. Hodnebrog, G. Myhre, Trends in atmospheric methane concentrations since 1990 were driven and modified by anthropogenic emissions, Commun. Earth Environ. 4 (2023) 317, https://doi.org/10.1038/s43247-023-00969-1.

[2] R. Haubrichs, R. Widmann, Evaluation of aerated biofilter systems for microbial methane oxidation of poor landfill gas, Waste Manag. 26 (2006) 408–416, https://doi.org/10.1016/j.wasman.2005.11.008.

[3] C.L. Souza, C.A.L. Chernicharo, S.F. Aquino, Quantification of dissolved methane in UASB reactors treating domestic wastewater under different operating conditions, Water Sci. Technol. 64 (2011) 2259–2264, https://doi.org/10.2166/wst.2011.695.

[4] B.C. Crone, J.L. Garland, G.A. Sorial, L.M. Vane, Significance of dissolved methane in effluents of anaerobically treated low strength wastewater and potential for recovery as an energy product: A review, Water Res. 104 (2016) 520–531, https://doi.org/10.1016/j.watres.2016.08.019.

[5] L. Fjelsted, C. Scheutz, A.G. Christensen, J.E. Larsen, P. Kjeldsen, Biofiltration of diluted landfill gas in an active loaded open-bed compost filter, Waste Manag. 103 (2020) 1–11, https://doi.org/10.1016/j.wasman.2019.12.005.

[6] T.L. Gómez-Borraz, A. González-Sánchez, W. Bonilla-Blancas, S. Revah, A. Noyola, Characterization of the biofiltration of methane emissions from municipal anaerobic effluents, Process Biochem. 63 (2017) 204–213, https://doi.org/10.1016/j.procbio.2017.08.011.

[7] N. Matsuura, M. Hatamoto, H. Sumino, K. Syutsubo, T. Yamaguchi, A. Ohashi, Recovery and biological oxidation of dissolved methane in effluent from UASB treatment of municipal sewage using a two-stage closed downflow hanging sponge system, J. Environ. Manag. 151 (2015) 200–209, https://doi.org/10.1016/j.jenvman.2014.12.026.

[8] J.L. Campos, D. Valenzuela-Heredia, A. Pedrouso, A. Val Del Río, M. Belmonte, A. Mosquera-Corral, Greenhouse gases emissions from wastewater treatment plants: minimization, treatment, and prevention, J. Chem. 2016 (2016), https://doi.org/10.1155/2016/3796352.

[9] U. Mrudulakumari Vasudevan, D.H.A. Mai, S. Krishna, E.Y. Lee, Methanotrophs as a reservoir for bioactive secondary metabolites: pitfalls, insights and promises, Biotechnol. Adv. 63 (2023) 108097, https://doi.org/10.1016/j.biotechadv.2023.108097.

[10] T. Sarat Chandra, R.S. Deepak, M. Maneesh Kumar, S. Mukherji, V.S. Chauhan, R. Sarada, S.N. Mudliar, Evaluation of indigenous fresh water microalga Scenedesmus obtusus for feed and fuel applications: effect of carbon dioxide, light and nutrient sources on growth and biochemical characteristics, Bioresour. Technol. 207 (2016) 430–439, https://doi.org/10.1016/j.biortech.2016.01.044.

[11] S.G. Hays, W.G. Patrick, M. Ziesack, N. Oxman, P.A. Silver, Better together: engineering and application of microbial symbioses, Curr. Opin. Biotechnol. 36 (2015) 40–49, https://doi.org/10.1016/j.copbio.2015.08.008.

[12] Z. Rasouli, B. Valverde-Pérez, M. D'Este, D. De Francisci, I. Angelidaki, Nutrient recovery from industrial wastewater as single cell protein by a co-culture of green microalgae and methanotrophs, Biochem. Eng. J. 134 (2018) 129–135, https://doi.org/10.1016/j.bej.2018.03.010.

[13] X. Li, Y. Lu, N. Li, Y. Wang, R. Yu, G. Zhu, R.J. Zeng, Mixotrophic cultivation of microalgae using biogas as the substrate, Environ. Sci. Technol. 56 (2022) 3669–3677, https://doi.org/10.1021/acs.est.1c06831.

[14] E.A. Hill, W.B. Chrisler, A.S. Beliaev, H.C. Bernstein, A flexible microbial co-culture platform for simultaneous utilization of methane and carbon dioxide from gas feedstocks, Bioresour. Technol. 228 (2017) 250–256, https://doi.org/10.1016/j.biortech.2016.12.111.

[15] R. Sander, Compilation of Henry's Law Constants for Inorganic and Organic Species of Potential Importance in Environmental Chemistry, 1999. ⟨http://www.mpch-mainz.mpg.de/~sander/res/henry.html⟩.

[16] K.M. Steel, K. Alizadehhesari, R.D. Balucan, B. Bašić, Conversion of CO_2 into mineral carbonates using a regenerable buffer to control solution pH, Fuel 111 (2013) 40–47, https://doi.org/10.1016/j.fuel.2013.04.033.

[17] W. Klinthong, Y.H. Yang, C.H. Huang, C.S. Tan, A Review: Microalgae and their applications in CO_2 capture and renewable energy, Aerosol Air Qual. Res. 15 (2015) 712–742, https://doi.org/10.4209/aaqr.2014.11.0299.

[18] V.M. Anusree, B.S. Sujitha, J. Anand, M. Arumugam, Dissolved inorganic carbonate sustain the growth, lipid and biomass yield of Scenedesmus quadricauda under nitrogen starved condition, Indian J. Exp. Biol. 55 (2017) 702–710.

[19] S. Cantera, V. Phandanouvong-Lozano, C. Pascual, P.A. García-Encina, R. Lebrero, A. Hay, R. Muñoz, A systematic comparison of ectoine production from upgraded biogas using Methylomicrobium alcaliphilum and a mixed haloalkaliphilic consortium, Waste Manag. 102 (2020) 773–781, https://doi.org/10.1016/j.wasman.2019.11.043.

[20] C. Tays, M.T. Guarnieri, D. Sauvageau, L.Y. Stein, Combined effects of carbon and nitrogen source to optimize growth of proteobacterial methanotrophs, Front. Microbiol. 9 (2018), https://doi.org/10.3389/fmicb.2018.02239.

[21] J.P. Bowman, Methylococcaceae, in: Bergey's Manual of Systematics of Archaea and Bacteria, Wiley, 2016, pp. 1–8, https://doi.org/10.1002/9781118960608.fbm00225.pub2.

[22] S. Mandal, J.B. Shurin, R.A. Efroymson, T.J. Mathews, Functional divergence in nitrogen uptake rates explains diversity–productivity relationship in microalgal communities, Ecosphere 9 (2018), https://doi.org/10.1002/ecs2.2228.

[23] J. Cabello, A. Toledo-Cervantes, L. Sánchez, S. Revah, M. Morales, Effect of the temperature, pH and irradiance on the photosynthetic activity by Scenedesmus obtusiusculus under nitrogen replete and deplete conditions, Bioresour. Technol. 181 (2015) 128–135, https://doi.org/10.1016/j.biortech.2015.01.034.

[24] P. Ruiz-Ruiz, T.L. Gómez-Borraz, S. Revah, M. Morales, Methanotroph-microalgae co-culture for greenhouse gas mitigation: effect of initial biomass ratio and methane concentration, Chemosphere 259 (2020), https://doi.org/10.1016/j.chemosphere.2020.127418.

[25] A. Toledo-Cervantes, M. Morales, E. Novelo, S. Revah, Carbon dioxide fixation and lipid storage by Scenedesmus obtusiusculus, Bioresour. Technol. 130 (2013) 652–658, https://doi.org/10.1016/j.biortech.2012.12.081.

[26] M. Dubois, K.A. Gilles, J.K. Hamilton, P.A. Rebers, F. Smith, Colorimetric method for determination of sugar and related substances, Anal. Chem. 28 (1956) 350–356, https://doi.org/10.1021/ac60111a017.

[27] S.K. Mishra, W.I. Suh, W. Farooq, M. Moon, A. Shrivastav, M.S. Park, J.W. Yang, Rapid quantification of microalgal lipids in aqueous medium by a simple colorimetric method, Bioresour. Technol. 155 (2014) 330–333, https://doi.org/10.1016/j.biortech.2013.12.077.

[28] M.E. Acuña, F. Pérez, R. Auria, S. Revah, Microbiological and kinetic aspects of a biofilter for the removal of toluene from waste gases, Biotechnol. Bioeng. 63 (1999) 175–184, https://doi.org/10.1002/(SICI)1097-0290(19990420)63:2<175::AID-BIT6>3.0.CO;2-G.

[29] D. He, L. Zhang, M.G. Dumont, J.S. He, L. Ren, H. Chu, The response of methanotrophs to additions of either ammonium, nitrate or urea in alpine swamp meadow soil as revealed by stable isotope probing, FEMS Microbiol. Ecol. 95 (2019), https://doi.org/10.1093/femsec/fiz077.

[30] Y. Zheng, L.M. Zhang, J.Z. He, Immediate effects of nitrogen, phosphorus, and potassium amendments on the methanotrophic activity and abundance in a Chinese paddy soil under short-term incubation experiment, J. Soils Sediment. 13 (2013) 189–196, https://doi.org/10.1007/s11368-012-0601-2.

[31] N. Yang, F. Lü, P. He, L. Shao, Response of methanotrophs and methane oxidation on ammonium application in landfill soils, Appl. Microbiol. Biotechnol. 92 (2011) 1073–1082, https://doi.org/10.1007/s00253-011-3389-x.

[32] S. Hoefman, D. Van Der Ha, N. Boon, P. Vandamme, P. De Vos, K. Heylen, Niche differentiation in nitrogen metabolism among methanotrophs within an operational taxonomic unit, BMC Microbiol. 14 (2014), https://doi.org/10.1186/1471-2180-14-83.

[33] G. Nyerges, L.Y. Stein, Ammonia cometabolism and product inhibition vary considerably among species of methanotrophic bacteria, FEMS Microbiol. Lett. 297 (2009) 131–136, https://doi.org/10.1111/j.1574-6968.2009.01674.x.

[34] Y. Yang, T. Tong, J. Chen, Y. Liu, S. Xie, Ammonium Impacts Methane Oxidation and Methanotrophic Community in Freshwater Sediment, Front. Bioeng. Biotechnol. 8 (2020), https://doi.org/10.3389/fbioe.2020.00250.

[35] S. Rossi, R. Díez-Montero, E. Rueda, F. Castillo Cascino, K. Parati, J. García, E. Ficara, Free ammonia inhibition in microalgae and cyanobacteria grown in wastewaters: photo-respirometric evaluation and modelling, Bioresour. Technol. 305 (2020), https://doi.org/10.1016/j.biortech.2020.123046.

[36] N. Roberts, M. Hilliard, Q.P. He, J. Wang, A microalgae-methanotroph coculture is a promising platform for fuels and chemical production from wastewater, Front. Energy Res. 8 (2020), https://doi.org/10.3389/fenrg.2020.563352.

[37] A.S. Safitri, J. Hamelin, R. Kommedal, K. Milferstedt, Engineered methanotrophic syntrophy in photogranule communities removes dissolved methane, Water Res. X 12 (2021), https://doi.org/10.1016/j.wroa.2021.100106.

[38] L.M. González-González, L.E. De-Bashan, Toward the enhancement of microalgal metabolite production through microalgae–bacteria consortia†, Biology 10 (2021) https://doi.org/10.3390/biology10040282.

[39] A. Ho, K. De Roy, O. Thas, J. De Neve, S. Hoefman, P. Vandamme, K. Heylen, N. Boon, The more, the merrier: heterotroph richness stimulates methanotrophic activity, ISME J. 8 (2014) 1945–1948, https://doi.org/10.1038/ismej.2014.74.

[40] A.J. Veraart, P. Garbeva, F. Van Beersum, A. Ho, C.A. Hordijk, M. Meima-Franke, A.J. Zweers, P.L.E. Bodelier, Living apart together - bacterial volatiles influence methanotrophic growth and activity, ISME J. 12 (2018) 1163–1166, https://doi.org/10.1038/s41396-018-0055-7.

[41] J. Park, H.F. Jin, B.R. Lim, K.Y. Park, K. Lee, Ammonia removal from anaerobic digestion effluent of livestock waste using green alga Scenedesmus sp, Bioresour. Technol. 101 (2010) 8649–8657, https://doi.org/10.1016/j.biortech.2010.06.142.

[42] J. Gutierrez, T.A. Kwan, J.B. Zimmerman, J. Peccia, Ammonia inhibition in oleaginous microalgae, Algal Res. 19 (2016) 123–127, https://doi.org/10.1016/j.algal.2016.07.016.

[43] E. Sforza, M. Pastore, S.M. Franke, E. Barbera, Modeling the oxygen inhibition in microalgae: an experimental approach based on photorespirometry, New Biotechnol. 59 (2020) 26–32, https://doi.org/10.1016/j.nbt.2020.06.003.

[44] J. Cabello, M. Morales, S. Revah, Dynamic photosynthetic response of the microalga Scenedesmus obtusiusculus to light intensity perturbations, Chem. Eng. J. 252 (2014) 104–111, https://doi.org/10.1016/j.cej.2014.04.073.

[45] K.K. Miroshnikov, S.E. Belova, S.N. Dedysh, Genomic determinants of phototrophy in methanotrophic alphaproteobacteria, Microbiology 88 (2019) 548–555.

[46] E. Broman, R. Barua, D. Donald, F. Roth, C. Humborg, A. Norkko, T. Jilbert, S. Bonaglia, F.J.A. Nascimento, No evidence of light inhibition on aerobic methanotrophs in coastal sediments using eDNA and eRNA, Environ. DNA 5 (2023) 766–781, https://doi.org/10.1002/edn3.441.

[47] H. Lee, J.I. Baek, J.Y. Lee, J. Jeong, H. Kim, D.H. Lee, D.M. Kim, S.G. Lee, Syntrophic co-culture of a methanotroph and heterotroph for the efficient

conversion of methane to mevalonate, Metab. Eng. 67 (2021) 285–292, https://doi.org/10.1016/j.ymben.2021.07.008.

[48] Y. Song, X. Wang, H. Cui, C. Ji, J. Xue, X. Jia, R. Ma, R. Li, Enhancing growth and oil accumulation of a palmitoleic acid–rich Scenedesmus obliquus in mixotrophic cultivation with acetate and its potential for ammonium-containing wastewater purification and biodiesel production, J. Environ. Manag. 297 (2021), https://doi.org/10.1016/j.jenvman.2021.113273.

[49] G. Flores-Salgado, F. Thalasso, G. Buitrón, M. Vital-Jácome, G. Quijano, Kinetic characterization of microalgal-bacterial systems: contributions of microalgae and heterotrophic bacteria to the oxygen balance in wastewater treatment, Biochem. Eng. J. 165 (2021), https://doi.org/10.1016/j.bej.2020.107819.